

Evaluating the Thermal Condition of Electrical Equipment via IRT Image Analysis

^{1,2}Mohd Shawal Jadin, ²Soib Taib, ³Suriadi

¹Faculty of Electrical and Electronic Engineering, Universiti Malaysia Pahang, 26600 Pekan, Pahang, Malaysia; ²School of Electrical and Electronic Engineering, Universiti Sains Malaysia, Engineering Campus 14300 Nibong Tebal, Seberang Perai Selatan, Pulau Pinang, Malaysia; ³Teknik Elektro, Universitas Syiah Kuala, Jl. Syech Abdul Rauf No.7 Darussalam Banda Aceh, Indonesia; Corresponding Author: mohdshawal@ump.edu.my

Abstract. The integrity of electrical power equipment is of paramount importance when it supplies electricity throughout a facility. However, the reliability of the equipments will degraded after sometime, and appropriate maintenance has to be taken accordingly to avoid future faults. Infrared thermography (IRT) image analysis is a commonly used technique for diagnosing the reliability of electrical equipments. Conventionally, the analysis of infrared image is done manually and takes very long time for further analysis. This paper proposes an automatic thermal fault detection and classification system for evaluating the condition of electrical equipment by analyzing its infrared image. First, the image is segmented to find the target region of interest (ROI). The detected regions which have the same region properties are grouped together in order to remove the unwanted regions. Finally, statistical features from each detected region are extracted and classified using the support vector machine (SVM) algorithm. The thermal condition of electrical equipments is evaluated based on qualitative measurement technique. The experimental result shows that the proposed system can detect and classify the thermal condition of electrical equipments.

Keywords: Infrared thermography, qualitative measurement, support vector machine.

Introduction

IRT technology is one of the useful tools for examining the condition of electrical installations. It offers a lot of advantages over conventional temperature measurement technique, including non-contact measurement, fast response time, wide temperature ranges, two-dimensional data acquisition, high spatial resolution, safe, reliable and very cost-effective (Hellier, 2001; Ghali *et al.*, 2011). The inspection can be done without interrupting the electrical system operation. Various problems can be detected especially in the central power installations of buildings and local switchboards. Within this unit where poor connections, short-circuits, overloads, load imbalances, improperly installed electrical components, etc. can be easily identified (Balaras & Argiriou, 2002).

However, to assess the condition of electrical equipments by analyzing IRT image can only be done by well-qualified and experienced personnel. In addition, the complete procedure of analyzing the infrared image is also time-consuming and costly. Therefore, to overcome these constraints, an automated infrared image analysis technique is employed through which the thermal anomalies within electrical equipment can be detected and evaluated quickly and accurately.

Research on automatic diagnostic the reliability of electrical equipments using IRT has been ongoing for many years (Jadin & Taib, 2012). Up to now, only few works on the advanced diagnostic system have been published. Based on the previous studies, the simplest method of identifying the hot spot regions within an IRT image of electrical equipment is to use thresholding techniques where the hot spot area is detected by filtering the image using a certain threshold value (Baoshu *et al.*, 2006; de Oliveira & Lages, 2010; Rahmani *et al.*, 2010; Ying-Chieh Chou & Yao, 2009). The hot region can be extracted using morphological segmentation where the maximum gray pixel value determines the maximum temperature of the hot region. The reference temperature is derived from the average gray values of the similar equipment outside the hot region. The condition of the equipment is evaluated by comparing the temperature difference between the hot spot and reference region (Ying-Chieh Chou & Yao, 2009).

In another research, an intelligent diagnostic system was developed to enable the detection and diagnosis of faults in surge arresters (Laurentys Almeida *et al.*, 2009). The image of a surge arrester was segmented using watershed transform. In this research, a neuro-fuzzy classifier was employed to classify the condition of the surge arrester. Korendo and Florkowski (Korendo & Florkowski, 2001) used invariant coefficient method to diagnose faults in power equipment. Rahmani (Rahmani *et al.* 2010) and Li (Baoshu *et al.*, 2006) employed moment features of the segmented hot regions and classify the equipment's condition by using the support vector machine (SVM). Shafi'i and Hamzah (Shafi'i & Hamzah, 2010) proposed an intelligent system to detect thermal anomaly in electrical equipment by using RGB colour data of infrared image and classify the image using the neural network. Although this method is quite straightforward, however, it has a problem with high processing time due to large feature vectors to be computed by a neural network. Lin *et al.* (Lin *et al.*, 2010) implemented image registration based on phase correlation and feature points matching for monitoring the thermal anomaly in electrical equipment.

This paper proposes a new method for diagnosing the reliability of electrical equipment by analyzing its infrared image. The thermal condition is evaluated based on qualitative measurement technique where the problematic parts of the equipment are compared with the normal one. The remainder of this paper is organized as follows: the next section briefly reviews the related works and followed by the proposed method. The next part presents the experimental results and discussions. Finally concluding remarks appeared in the last section of this paper.

Materials and Methods

There are two ways to analyze the thermal characteristics in electrical equipment. The first is quantitative measurement, which is to measure the exact real temperature value of an object. However, this measurement is relatively difficult to obtain. In order to determine the real and accurate temperature value, the true emissivity value must be identified by considering the effects of ambient conditions and atmospheric attenuation (dos Santos *et al.*, 2008). The second technique is to use qualitative measurement, which considers the relative temperature value of a particular hot spot with respect to a reference in that equipment. A hot spot is the abnormal component and the reference must be the similar component under the same condition. This method is widely used for evaluating the condition of electrical equipment (Lindquist *et al.*, 2005).

In order to analyze the condition of electrical installations automatically, image-processing technique is used to extract the thermal information within the infrared image. Image processing technique generally consists of several steps: segmentation (for finding ROIs), feature extraction, classification and decision (Solomon, 2011). The straightforward approach is to follow these steps one by one in bottom-up order. The general process of the system is shown Figure 1. Region segmentation process is the primary step for detecting ROIs. This stage is very critical since the classification performance is depending on the correct ROIs detection. The final regions segmentation is applied on the original infrared image in order to extract the thermal properties of the equipments. The local features such as the actual maximum temperature value and statistical thermal information for each detected region are extracted. Finally, all the extracted features are classified using SVM classifier in order to determine whether the equipment in normal or faulty condition. The accuracies of both classifiers are compared and evaluated. The method used in this study is based on qualitative measurement technique where all the similar equipments or similar components are compared to each other.

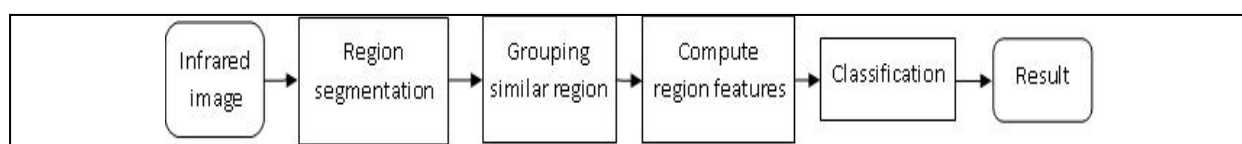


Figure 1. Block diagram of proposed system

Region segmentation

The aim of segmentation process is to separate the target hot spots of the electrical equipments from its background image. In this study, transition region extraction (TRE) was implemented to find the target ROIs. Transition in the target area is surrounded around a certain width, within the rapid change of gray-scale region. The main idea of transition region based image segmentation algorithm is to extract its transition region (between the target and background). The peak of TRE pixel histogram is used as the gate of image segmentation limit. It is a threshold-based image segmentation method. As image segmentation by TRE can be threshold, and thus the transition area will directly affect the quality of the extracted image segmentation quality. The frequent change of gray level brings abundant information for transition region. Gradient is a good indicator for sudden change of gray level, but not suitable for measuring frequent change of gray level. It is found that local entropy is a good measure for frequent change of gray level, but cannot reflect the extent of gray level changes. Therefore, Li and Liu have developed gray level difference-based (GLD) TRE that considers not only the gray level changes of transition region, but also represents the extent of gray level changes, which is more suitable for describing the properties of transition region (Li & C. Liu, 2009). The following steps describe the segmentation steps based on the total absolute pixel differences of TRE. Given a local neighbourhood size, $\Omega(x,y)$ of an image, $I(i,j)$ the transition region of the image can be extracted by

$$G(i, j) = \begin{bmatrix} \Delta f(1,1) & \cdots & \Delta f(1, j) \\ \vdots & \ddots & \vdots \\ \Delta f(i,1) & \cdots & \Delta f(i, j) \end{bmatrix} \quad (1)$$

where $\Delta f(i,j)$ is the total absolute difference between each pixel and can be derived by

$$\Delta f(i, j) = \sqrt{f_{max}(i, j) + f_{min}(i, j)} \quad (2)$$

$$f_{max}(i, j) = \max \left\{ \left| I(i, j) - \sum_{y=1}^M \sum_{x=1}^N \Omega(x, y) \right| \right\} x, y \neq i, j \quad (3)$$

$$f_{min}(i, j) = \min \left\{ \left| I(i, j) - \sum_{y=1}^M \sum_{x=1}^N \Omega(x, y) \right| \right\} x, y \neq i, j \quad (4)$$

Here f_{max} and f_{min} are the maximum and minimum absolute differences of local neighbourhood respectively. The threshold value of the transition region of the image, E_T is determined by

$$E_T = \alpha \times \max \{ G(i, j) \} \quad (5)$$

where α is the control coefficient which is ranged between 0 to 1. E_T value is then used as the threshold for extracting the transition region from the original gray level image. The example of infrared images and their corresponding TRE segmentation results are shown in Figure 2. Once the result is obtained, the mean value of the gray level image of transition region is computed to find the final segmentation threshold. Finally, the use of the standard image morphological technique will improve the accuracy of region segmentation while some unwanted small regions outside the electrical equipment are being eliminated.

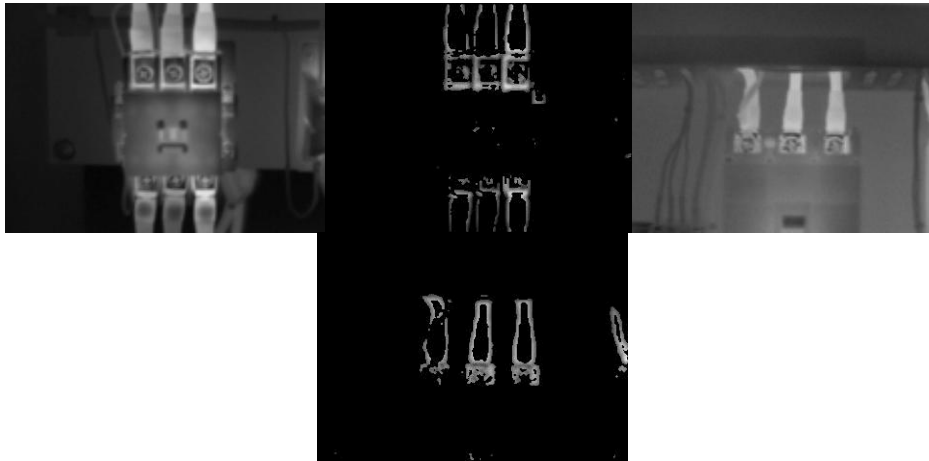


Figure 2. Infrared images and the result of TRE images

From segmentation results, it has shown that there are many unwanted regions, which are located outside the targeted ROIs. These regions should be discarded. For this purpose, grouping almost similar repetitive regions is the best approach for separating between the target regions and unwanted regions. So, certain features are given to each detected regions and it is considered as a group if the following criterions are fulfilled:

- Features distance between the regions.
- Spatial distance between two regions by calculating the distance between the centres of gravity of the regions.

Therefore, each segmented region is fitted with ellipse properties as the region features. Therefore, the first and second moments of the regions are computed. The first-order moments locate the centre of the ellipse and thus the position of the point of interest. For a region of $R = \{(x_i, y_i), i = 0, 1, 2, \dots, N\}$, the first-order moments are calculated by

$$m_{00} = \sum_x \sum_y I(x, y) dx dy \quad (6)$$

$$m_{10} = \sum_x \sum_y x I(x, y) dx dy \quad (7)$$

$$m_{01} = \sum_x \sum_y y I(x, y) dx dy \quad (8)$$

Then the second-order moments are calculated to find the orientation and the length of the axes of the ellipse which is given by

$$m_{x,x} = \frac{1}{N} \sum_{i=0}^N (x_i - \bar{x})^2 \quad (9)$$

$$m_{x,y} = \frac{1}{N} \sum_{i=0}^N (x_i - \bar{x})(y_i - \bar{y}) \quad (10)$$

$$m_{y,y} = \frac{1}{N} \sum_{i=0}^N (y_i - \bar{y})^2 \quad (11)$$

Here (\bar{x}, \bar{y}) is the centre of mass which is given by

$$\bar{x} = \frac{m_{10}}{m_{00}}, \bar{y} = \frac{m_{01}}{m_{00}} \quad (12)$$

The calculated moments are put in the matrix M form and diagonalized with matrix P .

$$M = \begin{bmatrix} m_{x,x} & m_{x,y} \\ m_{x,y} & m_{y,y} \end{bmatrix} \quad (13)$$

$$M = P \begin{bmatrix} \lambda_1 & 0 \\ 0 & \lambda_2 \end{bmatrix} P^{-1} \quad (14)$$

where

$$P = \begin{bmatrix} \cos \theta & -\sin \theta \\ \sin \theta & \cos \theta \end{bmatrix} \text{ and } \lambda_1 \geq \lambda_2 \quad (15)$$

λ_1 is the length of the first axis of the ellipse and λ_2 is the length of the second axis of the ellipse. θ is the angle formed by the abscissa axis and the first axis of the ellipse.

Grouping similar region

After fitting an ellipse, the minimum and maximum radiuses of the ellipse are taken out as the region features. Then all the similar features are matched together to form a group of repeated structures. This can be achieved by calculating the feature distances between two regions, where the nearest distance below a certain threshold value will receive the highest voting for both regions to be paired. Let R_i be all the detected regions where $i = 1, 2, \dots, L$, the degree of region similarities based on the ellipse properties can be defined as

$$t_{low} < \sum_{i=1}^L \left\{ \frac{f_{l_i}}{f_{l_{i+1}}}, \frac{f_{s_i}}{f_{s_{i+1}}} \right\} \leq t_{high} \quad (16)$$

where f_{l_i} and f_{s_i} are the minimum and maximum radiuses of the ellipse in region i while $f_{l_{i+1}}$ and $f_{s_{i+1}}$ are the minimum and maximum radiuses of the ellipse in region $i+1$. The value of t_{high} and t_{low} are the lower and upper threshold which set at in the ranges of ± 5 %. The ideal shape matching between two regions would produce the degree of similarities of 1. Figure 3 illustrates an example of region matching after fitting an ellipse. In this example, two groups of similar regions were detected. The first group consists of region label of 2, 5, 8 and 11 while the second group enclosed with the region label of 3, 6, 7 and 9.

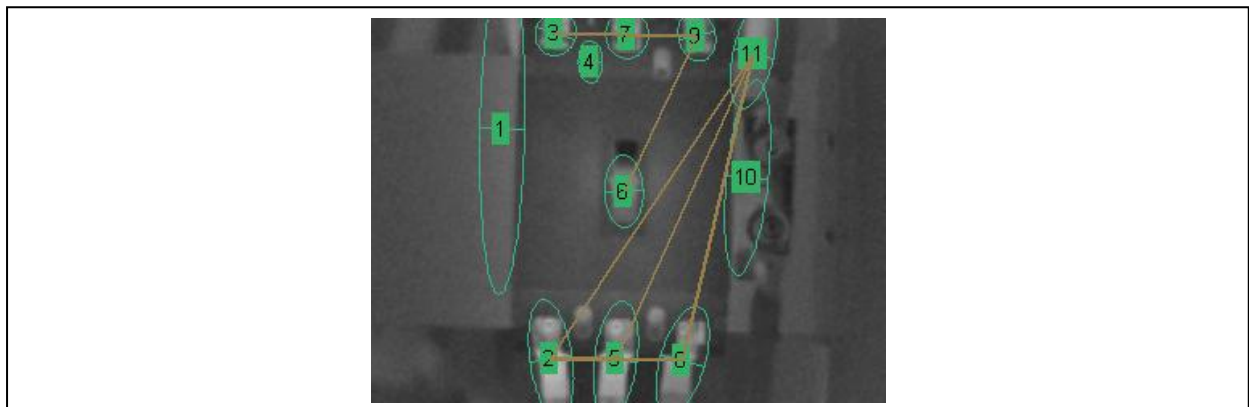


Figure 3. Matching of similar region

The region's grouping is limited at a certain spatial distance between two regions. The regions are considered as one group if they are located below a specific threshold value. Therefore, the distances between the two regions are calculated between the centres of gravity of the regions coordinate, which is given as

$$\sqrt{(c_i(x) - c_{i+1}(x))^2 + (c_i(y) - c_{i+1}(y))^2} \leq t_g \quad (17)$$

where c_i and c_{i+1} are the coordinates between region i and $i+1$ respectively. t_g is the threshold value through which the regions are considered as a group if the distance is below this threshold.

Feature extraction

Since, infrared images are represented in grayscale values, they do not show the actual temperature values. Therefore, the real temperature values of the image should be calculated. Each pixel of the image represents a certain temperature value. So, the actual temperature, T_r for each pixel is given by

$$T_r = T_{min} + \frac{T_{gray}}{T_{mgv}} \times (T_{max} - T_{min}) \quad (18)$$

The value of T_{max} and T_{min} representing the temperature range within the image. These temperature values can be obtained from thermal imagers. T_{gray} is the pixel intensity value at a certain point in the grayscale image while T_{mgv} is the highest grayscale value of the image. Table 1 summarized all the statistical thermal properties which were used to extract from each detected region. For each detected region, the number of pixels at gray level i is denoted as T_{ri} and N is the total number of pixels within the region. Maximum temperature of a region is determined by finding its maximum pixel and calculates using (18). Another important temperature measurement is the relative temperature differences between ROIs and background temperature. This information is useful in the case of all phases of electrical equipments showing the same thermal properties. Therefore, relative temperature difference, ΔT_{bg} between ROIs and background temperature can be used to determine the degree of temperature elevated from its normal condition.

Table 1. Statistical thermal parameters.

Name	Formula
Maximum temperature	$T_{mx} = T_{i_{max}}$
Average temperature	$T_{\mu} = \frac{1}{N} \sum_{i=1}^N T_{ri}$
Maximum temperature difference between region	$\Delta T_{reg} = T_{mx} - T_{other_region}$
Temperature relative to background	$\Delta T_{bg} = T_{mx} - T_{bg}$
Temperature standard deviation	$T_{\sigma} = \sqrt{\frac{1}{N-1} \sum_{i=1}^N (T_{ri} - T_{\mu})^2}$
Temperature skewness	$T_{Skewness} = \frac{1}{N} \sum_{i=1}^N \left(\frac{T_{ri} - T_{\mu}}{T_{\sigma}} \right)^3$
Temperature kurtosis	$T_{Kurtosis} = \frac{1}{N} \sum_{i=1}^N \left(\frac{T_{ri} - T_{\mu}}{T_{\sigma}} \right)^4$

Classification

In this paper, SVM was used for classifying the thermal condition of electrical equipment. All the extracted features are fed into both classifiers inputs for classification. The target output is to identify whether the electrical equipments is operating under normal or abnormal thermal condition. The performances of both classifiers are evaluated in terms of their accuracies. This section discusses about the principal of SVM classifiers.

SVM classifier is based on structural risk minimization principal from statistical learning theory (Vapnik 1999). It is a very useful technique for data classification and very efficient even for using a small number of training samples. It is very robust to handle large feature spaces and has a good generalization property compared to conventional classifiers. In classification process, SVM seeks to find an optimal separating hyper-plane or boundary by maximizing the margin between the separating feature spaces or classes as illustrated in Figure 4.

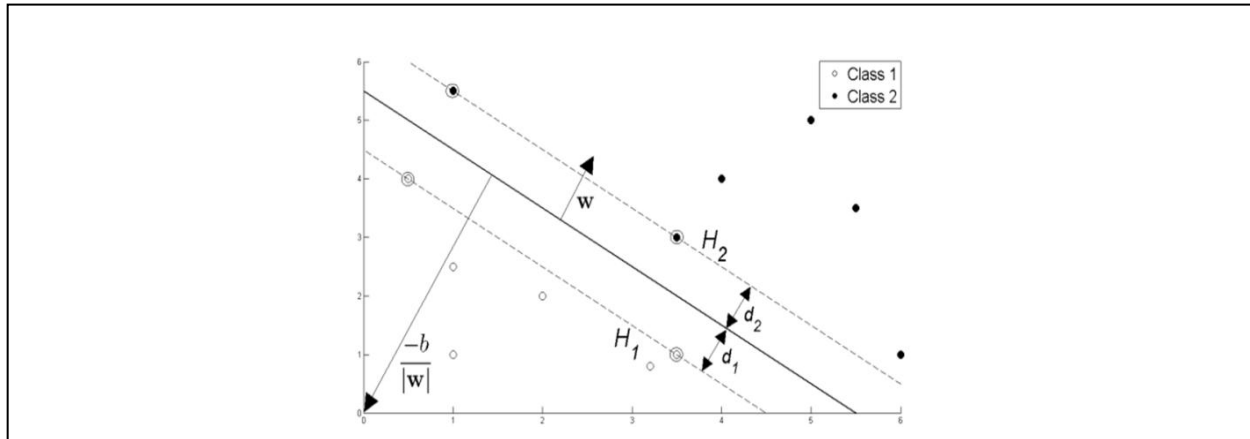


Figure 4. Hyper-plane through two linearly separable classes.

The resulting hyper-plane separation depends on training patterns called as support vector. If a set of input data with classification label (x_i, y_i) , $i = 1, 2, 3, \dots, M$ where M is the number of sample and $y_i \in \{1, -1\}$, the linear hyper-plane separation data can be determined by:

$$f(x) = w^T x + b = \sum_{j=1}^n w_j x_j + b = 0 \quad (24)$$

where w is an n -dimensional vector and b is a scalar. The vector w and the scalar b determined the position of the separating hyper-plane. The separating hyper-plane satisfies the following condition:

$$\begin{cases} w^T x_i + b \geq +1, & \text{if } y_i = +1 \\ w^T x_i + b \leq -1, & \text{if } y_i = -1 \end{cases} \quad (25)$$

which is equivalent to

$$y_i (w^T x_i + b) \geq +1 \quad \text{for } i = 1, 2, \dots, M \quad (26)$$

The optimal hyper-plane for separating the data can be determined by following optimization problem:

$$\text{Minimize } \frac{1}{2} \|\omega\|^2 + C \sum_{i=1}^M \xi_i \quad (27)$$

$$\text{Subject to } \begin{cases} y_i (w^T (x_i) + b) \geq 1 - \xi_i, & \text{for } i = 1, 2, \dots, M \\ \xi_i \geq 0, & \text{for all } i \end{cases} \quad (28)$$

where ξ_i is the measuring distance between the margin and the examples x_i which are lying on the wrong side of margin. C is the penalty parameter of the error. The kernel function is a method for using a linear classifier algorithm to solve a nonlinear problem by mapping the original nonlinear observations into a higher-dimensional space (Cristianini & Shawe-Taylor, 2000). If each of the training vectors x_i are mapped into a higher-dimensional space by the function $\phi(x_i)$, the kernel function used for nonlinear decision function is given as

$$y(x) = \text{sign} \left[\sum_{i=1}^M y_i K(x, x' + b) \right] \quad (29)$$

where $K(x, x')$ is the kernel function that returns a dot product of two vectors x and x' in the feature space mappings of the original data points, which is defined as

$$K(x, x') = \phi(x)^T \phi(x') \quad (30)$$

There are many types of functions can be used as a kernel. However, the basic kernel functions which have been successfully applied to a wide variety of applications are given in Table 2.

Table 2. Kernel functions.

Kernel	Formula
Linear	$K(x, x') = x \cdot x'$
Polynomial	$K(x, x') = (x \cdot x' + C)^d$
RBF	$K(x, x') = \exp\left(-\frac{\gamma(x - x')^2}{\sigma}\right)$
Sigmoid	$K(x, x') = \tanh(\gamma x \cdot x' + C)$

Results and Discussion

Infrared images were captured using Fluke Ti25 thermal imager with fusion technology. The thermal imager consisted of a 160 X 120 focal plane array, uncooled microbolometer detector and operated in the infrared spectral band of 7.5 μm to 14 μm . The thermal lens capture images of 320 x 240 pixels while the ordinary lens produced 640 x 480 pixels (visual images). All the infrared images of electrical equipments were collected at the main switchboards (MSB) which are supplying electricity to office buildings and paper mill factory. For capturing the image, the thermal imager orientation is directly facing to the target electrical equipments in order to get an accurate measurement. The distance between the target electrical equipment and the thermal imager is in the range of 0.5m - 1.0m. The thermal imager was calibrated before inspection and the emissivity value was set at 0.95 for all painted and black electrical equipments and components. Emissivity value has to be set correctly in order to get accurate temperature reading (McDaid & Y. Zhang, 2011). It was also noted that the ambient temperature around the equipments is between 30-33 $^{\circ}\text{C}$ during inspection.

Figure 5 depicts the examples of ROIs identification after rejecting unwanted regions and grouping the similar regions. The segmentation results are superimposed with the original grayscale images. The common type of faults such as poor electrical connection, overloading, load imbalance and some other faults have been tested for the image segmentation. Most of the images have been successfully segmented and ROIs were truly located. But in some cases ROIs did not give a satisfactory result due to high-intensity variation in the infrared image.

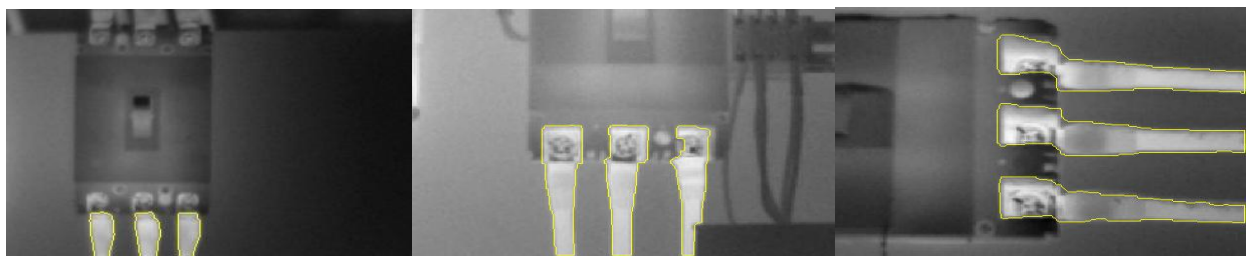


Figure 5. ROI identification results superimposed with the original image.

Classification performance analysis

In this stage, SVM algorithm is trained and tested with the above-mentioned kernel functions (linear, polynomial, RBF and sigmoid). Seven features extracted from 194 regions in 65 images, which were used as the inputs for both classifiers. All these data were divided into the training-set and test-set. The training data set was made up of randomly selected of 116 samples (60 %) and the remaining 78 samples (40 %) formed the testing data set. The performances of all classifiers are evaluated based on percentage of specificity, sensitivity, precision and accuracy, which are defined as follows:

$$\text{Sensitivity} = \frac{TF}{TF + FNF} \quad (31)$$

$$\text{Specificity} = \frac{TNF}{TF + FNF} \quad (32)$$

$$\text{Precision} = \frac{TF}{TF + FF} \quad (33)$$

$$\text{Accuracy} = \frac{TF + TNF}{TF + FF + TNF + FNF} \quad (34)$$

where, *TF* and *TNF* are correctly predicted abnormal and normal equipments respectively. In contrast, *FF* and *FNF* are false predicted normal and abnormal equipments correspondingly. Table 3 shows the training and testing results of SVM using different kernel functions. The training performance of SVM using linear, polynomial, RBF, sigmoid function are 99 %, 100 %, 99 % and 80 % respectively. On the other hand, the testing result produces 95.745 %, 91.489 %, 79.787 % and 71.277 % in that order. Obviously, SVM classifier using linear kernel function provides the best performance with overall accuracy of 97.423 %.

Table 3. Overall training and testing accuracies of SVM classification using different Kernel functions.

Kernel	Training (%)	Testing (%)	Overall (%)
Linear	99	95.745	97.423
Polynomial	100	91.489	95.876
RBF	99	79.787	89.691
Sigmoid	80.000	71.277	75.773

Conclusions

In this paper, an advanced method for detecting and classifying the thermal condition of electrical equipment based on qualitative infrared image analysis had been proposed. An image segmentation approach based on TRE and ROI identifications by grouping the similar regions within an infrared image is introduced. Seven statistical thermal features are extracted from each ROI as the input parameters for the classifier. Experimental results show that SVM classifier using linear kernel function gives the best performance compared to other kernel functions with the accuracy of 97.423 %. It is important to note that the accuracy of classification is depending on correct ROIs detection. Therefore, a better method of segmentation should be adopted for finding better ROIs detection and thus produce better classification accuracy.

Acknowledgements

The authors gratefully acknowledge University Sains Malaysia under Postgraduate Research Grant Scheme (USM-RU-PRGS: 1001/PELECT/8043058) and University Malaysia Pahang for their financial support and facilities.

References

- Balaras C.A., Argiriou A.A. 2002. Infrared thermography for building diagnostics. *Energy and Buildings*, 34(2), pp.171–183.
- Baoshu Li *et al.*, 2006. HV power equipment diagnosis based on infrared imaging analyzing. *International Conference on Power System Technology*, pp 1–4.
- Cristianini N., Shawe-Taylor J. 2000. *An Introduction to Support Vector Machines and Other Kernel-based Learning Methods*, 1st ed. Cambridge University Press.
- Ghali V.S., Mulaveesala R., Takei M. 2011. Frequency-modulated thermal wave imaging for non-destructive testing of carbon fiber-reinforced plastic materials. *Measurement Science and Technology*, 22(10):104018.
- Hellier C. 2001. *Handbook of Nondestructive Evaluation*, 1st edition. McGraw-Hill Professional, USA.

- Jadin M.S., Taib S. 2012. Recent progress in diagnosing the reliability of electrical equipment by using infrared thermography. *Infrared Physics & Technology*, 55(4):236–245.
- Korendo Z., Florkowski M. 2001. Thermography based diagnostics of power equipment. *Power Engineering Journal*. 15(1):33–42.
- Laurentys Almeida C.A. *et al.* 2009. Intelligent thermographic diagnostic applied to surge arresters: A new approach. *IEEE Transactions on Power Delivery*, 24(2):751–757.
- Li Z., Liu C. 2009. Gray level difference-based transition region extraction and thresholding. *Computers & Electrical Engineering*, 35(5):696–704.
- Lin L. *et al.* 2010. A substation infrared temperature monitoring and warning system with object separation and image registration. *International Conference on Image Processing and Pattern Recognition in Industrial Engineering*, Xi'an, China, pp 78202B–78202B–9.
- Lindquist T.M., Bertling L., Eriksson R. 2005. Estimation of disconnecter contact condition for modelling the effect of maintenance and ageing. In *Power Tech, Russia*, pp 1–7.
- McDaid C., Zhang Y. 2011. Wall temperature measurements using a thermal imaging camera with temperature-dependent emissivity corrections. *Measurement Science and Technology*, 22(12):125503.
- Meola C., Carlomagno G.M. 2004. Recent advances in the use of infrared thermography. *Measurement Science and Technology*, 15(9):R27–R58.
- de Oliveira J.H., Lages W.F. 2010. Robotized inspection of power lines with infrared vision. In *2010 1st International Conference on Applied Robotics for the Power Industry*, pp 1–6.
- Rahmani A., Haddadnia J., Seryasat O. 2010. Intelligent fault detection of electrical equipment in ground substations using thermo vision technique. In *International Conference on Mechanical and Electronics Engineering*, pp V2–150–V2–154.
- dos Santos L. *et al.* 2008. Infrared thermography applied for outdoor power substations. In V. P. Vavilov & D. D. Burleigh, eds. *Thermosense XXX*. Thermosense XXX. Orlando, FL, USA: SPIE, pp 69390R–11.
- Shafi'i M.A., Hamzah N. 2010. Internal fault classification using Artificial Neural Network. In *4th International Conference on Power Engineering and Optimization (PEOCO)*, pp 352–357.
- Solomon C. 2011. *Fundamentals of digital image processing: a practical approach with examples in Matlab*, Wiley-Blackwell, Hoboken NJ.
- Vapnik V., 1999. *Nature of statistical learning theory*. Springer.
- Ying-Chieh C., Yao L. 2009. Automatic Diagnostic System of Electrical Equipment Using Infrared Thermography. In *International Conference of Soft Computing and Pattern Recognition*, pp 155–160.